High Affinity of the Cell-Penetrating Peptide HIV-1 Tat-PTD for DNA†

André Ziegler* and Joachim Seelig

Department of Biophysical Chemistry, Biozentrum, University of Basel, Kingelbergstrasse 50/70, 4056 Basel, Switzerland

Received March 1, 2007; Revised Manuscript Received May 4, 2007

ABSTRACT: During cellular uptake of fluorescently labeled cell-penetrating peptides (CPPs), intense fluorescent signals are commonly observed in the nucleus of the cell, suggesting intracellular CPP relocation and potential binding to the genome of the host. We therefore investigated the interaction of the CPP HIV-1 Tat(47−57) with double-stranded DNA, and we also tested whether the fluorescence intensity of the labeled CPP allows for linear predictions of its intracellular concentration. Using isothermal titration calorimetry, we observe that the CPP has a high affinity for salmon sperm DNA as characterized by a microscopic dissociation constant of 126 nM. The binding is exothermic, with a reaction enthalpy of −4.63 kcal/mol CPP (28 °C). The dissociation constant and reaction enthalpy decrease further at higher temperatures. The affinity of the CPP for DNA is thus 1−2 magnitudes higher than for extracellular heparan sulfate, the likely mediator of the CPP uptake. Accordingly, the high affinity for DNA confers stability to extracellular transport complexes of CPP and DNA but potentially affects the regulation and molecular organization of the host's genome after nuclear uptake. Moreover, the CPP leads to the condensation of DNA as evidenced by the pronounced increase in light-scattering intensity. The fluorescence quantum yield of the FITC-labeled CPP decreases considerably at concentrations > 5 μmol/L, at pH < 7, and upon binding to DNA and glycosaminoglycans. This change in fluorescence quantum yield impedes the microscopic identification of uptake routes and the comparison of uptake efficiency of different CPPs, especially if the accumulation in subcellular compartments (self-quenching and pH difference) and transitory binding partners (quenching and condensation) is unknown.

Cell-penetrating peptides (CPPs)[1] are molecules of commonly polycationic nature that traverse the membrane of biological cells within seconds to minutes (for a review, see ref *1*). During their cellular uptake, they can take other molecules such as plasmid DNA or enzymes along that would not cross the cell membrane otherwise. In analogy to other polycationic transfection reagents, such as poly-L-lysine (PLL) (*2*) and polyethylenimine (*3*), CPPs must not be linked covalently to the cargo as long as the binding affinity between CPP and cargo is sufficiently high to afford stability of the complex during transport and uptake. In addition, the molar ratio of the two compounds is decisive, because a net positive charge of the polyplex yields an optimum transfection efficiency (*4*).

To follow and compare the uptake of CPPs in living cells, these molecules are commonly conjugated to fluorescent dyes for observations with fluorescence microscopy or fluorescence-activated cell sorting (FACS). After cellular uptake of fluorescently labeled CPPs, major fluorescence signals are commonly observed in the cell nucleus (*5*). These observations raise the questions of whether the intense fluorescence signal in the nucleus actually represents binding of the CPP to the DNA of the host after its cellular uptake and whether the fluorescence intensity in the nucleus truly reflects the local CPP concentration.

Clearly, a *strong* affinity between CPP and cargo DNA is required to stabilize the resulting polyplex during transport and to achieve an optimum transfection yield. On the other hand, a sufficiently *low* affinity between CPP and cargo is required to facilitate the release of the cargo after its cellular uptake, as potentially achieved through enzymatic digestion of the CPP, pH differences, or competitive displacement of the cargo. In this context, the rapid appearance of labeled CPPs in the cell nucleus (*5*) suggests that the uptake of the CPP into the nucleus likely precedes its digestion.

This delicate balance between various binding affinities has important consequences, because the intracellular binding of CPPs to the genome of the host will lead to the release of the cargo but, at the same time, will create safety risks. A strong affinity for intracellular DNA commonly affects the regulation and molecular organization of the genome, which has not been considered in the few existing toxicity studies on CPPs (e.g., refs *5*−*11*). Knowing the binding affinity of the CPP for cargo molecules and for potential cellular binding sites is thus essential to understand the cellular fate, redistribution, and safety of CPPs.

We therefore investigated systematically the binding affinity of the HIV-1 Tat CPP to double-stranded DNA. The

† This work was supported by Swiss National Science Foundation Grant 3100-107793/1.

* To whom correspondence should be addressed: Biozentrum, University of Basel, Kingelbergstrasse 50/70, 4056 Basel, Switzerland. Telephone: +41-61-267 2180. Fax: +41-61-267-2189. E-mail: andre. ziegler@unibas.ch.

[1] Abbreviations: bp, base pair; CPP, cell-penetrating peptide; ds, double-stranded; EIAV, equine infectious anemia virus; FACS, fluorescence-activated cell sorting; FITC, fluorescein isothiocyanate; GAG, glycosaminoglycan; HIV-1, human immunodeficiency virus type 1; HS, heparan sulfate; ITC, isothermal titration calorimetry; PLL, poly-L-lysine; PTD, protein transduction domain; TAR, transacting responsive element; Tat, transacting transcriptional activator.

10.1021/bi700416h CCC: $37.00 © 2007 American Chemical Society
Published on Web 06/08/2007

cell-penetrating property ("transduction") of this protein essentially results from its basic epitope (amino acids 49−57) (*12*) that is also termed the protein transduction domain (Tat-PTD) (*1*). This epitope is also responsible for the binding of Tat to mRNA, which represents the intrinsic function of Tat in the nucleus of the guest cell. Accordingly, binding of Tat to the initial 5′ mRNA transcript (TAR) of the viral genome enhances its transcription by a factor of 100−1000 (*13*). This interaction has been found to be specific because of the core epitope (amino acids 19−42) (*13*), particular arginine residues in the basic epitope of Tat (*14, 15*), and particular nucleotides in TAR (*16*). The specific interaction of TAR with full-length Tat (*16, 17*), Tat(32−72) (*18*), and the basic epitope Tat(47−58) (*14, 19*) has been characterized by a dissociation constant of 6−70 nM. In contrast, no thermodynamic data for the HIV-1 Tat-PTD binding to DNA are available to the best of our knowledge. Moreover, because CPPs are often employed as fluorescently labeled derivatives, we tested whether the fluorescence signal of the CPP is linearly correlated to its concentration under various cellular conditions. This knowledge is essential for a quantitative interpretation of microscopic observations and the comparison of different CPPs.

EXPERIMENTAL PROCEDURES

Buffer. All reactions were carried out in aqueous solution using NaCl (76 mM) containing phosphate buffer (30 mM) at pH 7.40, yielding physiological ionic strength (154 mM). Results are reported as mean ± standard deviation from four individual sample preparations.

Materials. Double-stranded (ds) DNA (41% GC content) from salmon testes was purchased from Sigma-Aldrich (Buchs, Switzerland) and was sheared to strands with an average size of 2000 base pairs (bp) using a Branson tip sonifier (Danbury, CT) with 4 pulses (5 W/mL) of 15 s duration. The median melting temperature of these DNA strands in buffer was 84.9 °C (half-width = 8.2 °C) as measured with differential scanning calorimetry (Microcal VP-DSC calorimeter; Northampton, MA). The actual concentration of DNA was assessed spectrophotometrically using an extinction coefficient of 13 200 M $(bp)^{-1}$ cm^{-1} at 260 nm (*20*). Novasyn−TGA resin and (fluorenylmethoxy)-carbonyl (Fmoc)-protected amino acids were purchased from Nova Biochem (Läufelingen, Switzerland), and 5-fluorescein isothiocynanate (FITC) was purchased from Anaspec-Anawa (Wangen, Switzerland). Porcine intestinal mucosa heparin [sodium salt; sulfate content of 11.3%; average molecular weight (MW) of 13 000] was from Celsus Laboratories (Cincinnati, OH). All other chemicals of high-performance liquid chromatography (HPLC) grade were from Sigma-Aldrich (Buchs, Switzerland).

Peptide Synthesis. Solid-phase peptide synthesis of HIV-1 Tat-PTD (residues 47−57 of HIV-1 Tat; H_3N^+-YGRKKRRQRRR-COO^-) and fluorescein-labeled Tat-PTD (fluorescein-[βA]-GGGG-YGRKKRRQRRR-COO^-) was carried out on an Abimed EPS221 peptide synthesizer (Langenfeld, Germany) using Fmoc-protected amino acids. The fluorescein-labeled CPP was obtained by coupling 5-FITC to the N terminus of the crude peptide before deprotection of the Fmoc groups (*5*). After Fmoc deprotection, the peptides were purified by preparative high-pressure liquid chromatography. The mass of the peptides was confirmed by electrospray ionization mass spectrometry, and peptide purity (>98%) was assessed by analytical high-pressure liquid chromatography. The effective peptide concentration was measured as the amino acid content after acid hydrolysis.

Isothermal Titration Calorimetry (ITC). The heat flow resulting from the binding of the CPP to DNA was measured with high-sensitivity ITC using a Microcal VP-ITC calorimeter (Northampton, MA) with a reaction cell volume of 1.4 mL. The ITC data were evaluated according to the multisite binding model (*21*)

$$\frac{[\mathrm{CPP}]_\mathrm{b}}{[\mathrm{DNA}]_\mathrm{t}} = \frac{nK_i[\mathrm{CPP}]}{1 + K_i[\mathrm{CPP}]} \quad (1)$$

where $[CPP]_b$ and [CPP] are the concentrations of bound and free CPP, respectively, $[DNA]_t$ is the total concentration of the DNA, K_i is the microscopic binding constant to each individual binding site in the DNA, and n is the number of CPP molecules bound per DNA molecule. K_i, n, and the CPP-binding enthalpy, ΔH^0_{CPP}, may be directly determined by a three-parameter least-square fit to the calorimetric data. Typically, the reaction cell is filled with a CPP solution of 50 μM, and the DNA solution (1.41 mM bp) is injected with 10 μL aliquots. Accordingly, the heat released in injection i, δQ_i, is proportional to the concentration of bound CPP per injection by

$$\delta Q_i = \Delta H^0_{\mathrm{CPP}} \delta[\mathrm{CPP}]_{\mathrm{b},i} V \quad (2)$$

where $\delta[CPP]_{b,i}$ is the change in the bound ligand concentration upon injection i and V is the actual reaction volume. A noncooperative character for the CPP binding to DNA was assumed on the basis of experimental findings on the interaction of octalysine with DNA (*22*). For macromolecules such as DNA with n independent binding sites, the binding constant of the individual binding site varies with the degree of saturation for statistical reasons (*21*), with the first ligand binding with the macroscopic binding constant $K_1 = nK_i$ and the last ligand binding with the macroscopic binding constant $K_n = K_i/n$. For a better comparison with the literature, dissociation constants K_d are reported that are the inverse of the binding constants.

Static Right-Angle Light Scattering. Static light scattering at a right angle was measured with a Jasco FP 777 fluorimeter (Tokyo, Japan) set at a wavelength of 350 nm under constant stirring and at a temperature of 28 °C. Quartz cuvettes with inner lengths of 1 cm were filled with 1.4 mL of CPP solution, and 10 μL aliquots of the DNA solution were added in 5 min intervals.

Fluorescence. The fluorescence signal of the fluorescein-labeled CPP was measured with a Jasco FP 777 fluorimeter (Tokyo, Japan) at a wavelength set to maximum excitation (498 nm) and emission (521 nm) of fluorescein. Quartz cuvettes with inner lengths of 1 cm were used to measure volumes of 1.4 mL.

RESULTS

DNA Binding. The cell-penetrating peptide HIV Tat-PTD binds with high affinity to double-stranded DNA as evidenced by high-sensitivity ITC (Figure 1). In this experiment,

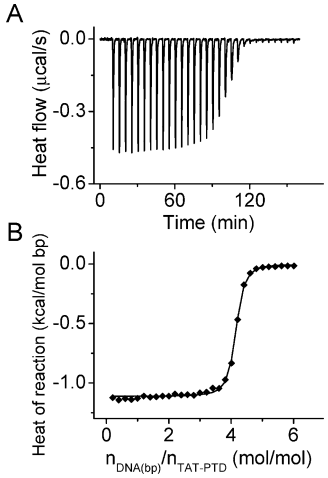

FIGURE 1: The CPP HIV-1 Tat-PTD binds to salmon sperm DNA as observed by ITC. The reaction cell (V_{cell} = 1.4037 mL) is filled with 50 μM HIV Tat-PTD. Every 5 min, 10 μL of a 1.41 mM (bp) salmon testes DNA is injected. (A) Experimental heat flow as a function of time as caused by the injections of DNA into Tat. (B) Heat of reaction h_i (=integral of the heat flow) as a function of the number of injections N_i. The ◆ represent experimental data. The solid line is a least-square fit using the binding model described by eqs 1 and 2, with the parameters listed in Table 1. The temperature was 28 °C. The buffer in all experiments was 30 mM phosphate and 76 mM NaCl at pH 7.40 (resulting in an ionic strength of 154 mM).

1.4 mL of a 50.0 μM solution of the CPP was titrated every 5 min with 10 μL of a 1.41 mM (bp) DNA solution. The DNA reacted rapidly with the CPP as evident from the heat flow as a function of time (Figure 1A). Integration of the titration peaks yields nearly identical amounts of heat released ($h_i \approx -16$ μcal) during the first 14 titrations (Figure 1B). In the subsequent 10 titrations, the heat of reaction continuously decreased, and this transition region is essential to evaluate the binding constant at given concentrations (see below). In the residual 6 injections, no substantial heats of reaction were detected any longer ($h_i \approx -0.3$ μcal) and were equal to injections of DNA into pure buffer (not shown), revealing that all binding sites of the CPP are saturated with DNA.

Even without assuming a specific binding model, these experimental data allow three quantitative conclusions. First, during the initial injections, the CPP is much in excess over the added DNA. The observed plateau region thus denotes that the added DNA is completely bound to the CPP. The molar heat of binding, ΔH^0_{DNA}, is thus given by $h_i/n_{i,DNA}$, where h_i is the heat of reaction per injection (≈ -16 μcal) and $n_{i,DNA}$ is the molar amount of DNA added in each injection (14.1 nmol bp). The evaluation of this plateau region thus yields $\Delta H^0_{DNA(bp)} = -1.192 \pm 0.038$ kcal/mol bp. This exothermic reaction contrasts with the binding of smaller cations such as divalent magnesium (*23*), trivalent cobalt hexammine $[Co(NH_3)_6]^{3+}$ (*24*), and tetravalent spermine (*23*) to DNA, where the binding is mainly endothermic (*24*). The present findings are, however, in agreement with the binding of larger cations such as PLL to DNA, where an exothermic reaction and comparable reaction enthalpy (−0.6 kcal/mol bp) was found (*23*).

Next, the molar heat of binding for the *peptide*, ΔH^0_{CPP}, can be calculated by $h_{i,tot}/n_{CPP,tot}$, where $h_{i,tot}$ is the sum of the reaction heat (≈ -315 μcal) and $n_{CPP,tot}$ is the molar amount of the peptide (70.2 nmol). This evaluation yields $\Delta H^0_{CPP} = -4.58 \pm 0.40$ kcal/mol CPP, which is similar to the reaction enthalpy of −4.9 kcal/mol of oligolysine binding to nucleic acids (*25*). Present ΔH^0_{CPP} values also correspond to the binding of CPPs to the glycosaminoglycan heparan sulfate, the likely mediator of the CPP uptake (*26*−*28*), where a $\Delta H^0_{CPP} = -4.6$ kcal/mol CPP was observed (*29*). The observed ΔH^0_{CPP} values for DNA binding are, however, lower than those found for the interaction of the CPP with heparin (*29*), the GAG species with the highest charge per disaccharide (*30*).

Assuming that most of the reaction enthalpy originates from the release of hydration water and related co-ions during DNA condensation (*20*, *31*), the ΔH^0_{CPP} values for CPP binding to DNA suggest that the condensation of the CPP is more pronounced with highly sulfated heparin (*29*) as compared to DNA. This is also supported by fluorescence data (see below). In contrast, the binding affinity is lower for the interaction of the CPP with low-sulfated heparan sulfate (*29*) as compared with DNA, with essential consequences for the optimum charge ratio of the transport complex (see the Discussion).

As the titration continues beyond the plateau region, the supply of Tat-PTD becomes exhausted and the titration peaks suddenly become smaller. The midpoint of this transition (e.g., injection number 21 in Figure 1) can be observed at a DNA(bp)/Tat-PTD molar ratio of $r_{DNA/CPP} = 4.14 \pm 0.34$. As a third quantitative conclusion, it follows that a Tat-PTD molecule binds on the average 4.14 DNA base pairs, leading essentially to charge neutralization when considering 8 positive charges for the CPP and 2 negative charges per DNA base pair at physiological pH.

A full thermodynamic description of the experiment can be obtained by assuming a multisite binding model, where a three-parameter fit of eq 2 is applied to the experimental data (Figure 1B). This procedure (Table 1) reveals again a reaction enthalpy of $\Delta H^0_{CPP} = -4.63 \pm 0.40$ kcal/mol CPP and a stoichiometry of $r = 4.00 \pm 0.26$ (at 28 °C) in agreement with the results obtained above without invoking a specific binding model. In addition, the fitting procedure yields important thermodynamic binding parameters (Table 1) such as the change in entropy ($T\Delta S^0 = +4.92 \pm 0.55$ kcal/mol CPP), dissociation constant ($K_{d,i} = 126 \pm 50$ nM), and free energy of binding ($\Delta G^0 = -9.56 \pm 0.31$ kcal/mol). The surprisingly high gain in entropy (degree of disorder) is expected to reflect the release of hydration water (*31*) and counter-ions (*25*) during polyelectrolyte binding and condensation, which is also supported by light-scattering data (see below).

Both negative ΔH^0_{CPP} and positive $T\Delta S^0$ are thus favorable to the overall binding reaction, and they are even more favorable at higher temperatures, as evident by repeating the experiment at different temperatures (Figure 2). Here, the entropy term changed only moderately over the entire temperature range of 40 °C (Figure 2), whereas ΔH^0_{CPP} decreased considerably at higher temperatures thus contributing to a more favorable free energy of binding, decreasing the dissociation constant at higher temperatures. This temperature dependence of ΔH^0_{CPP} is characterized by a negative molar heat capacity of $\Delta C^0_p = -54.2$ cal K^{-1} mol^{-1}. A negative heat capacity typically indicates that the binding

Table 1: Thermodynamic Binding Parameters for the Interaction of HIV-1 Tat-PTD^{8+} with Salmon Sperm DNA at Indicated Temperatures[a]

T (°C)	dissociation constant, $K_{d,i}$ (nM)	stoichiometry[b] (n_{bp}/n_{CPP})	reaction enthalpy, ΔH^0_{CPP} (kcal/mol CPP)	change in entropy, $T\Delta S^0$ (kcal/mol CPP)	change in free energy, ΔG^0 (kcal/mol complex)
8	238 ± 24	3.95 ± 0.18	−3.49 ± 0.18	5.03 ± 0.18	−8.52 ± 0.06
18	152 ± 4	4.02 ± 0.16	−4.08 ± 0.16	5.06 ± 0.17	−9.08 ± 0.01
28	126 ± 50	4.00 ± 0.26	−4.63 ± 0.40	4.92 ± 0.55	−9.56 ± 0.31
38	67 ± 4	4.54 ± 0.06	−5.45 ± 0.28	4.76 ± 0.28	−10.21 ± 0.01
48	79 ± 23	4.43 ± 0.19	−5.52 ± 0.39	4.94 ± 0.51	−10.46 ± 0.18

[a] Conditions used are isotonic buffer at pH 7.40 (76 mM NaCl and 30 mM sodium phosphate). [b] Stoichiometry as determined experimentally (ITC) for 100% of the binding sites of DNA saturated with the CPP.

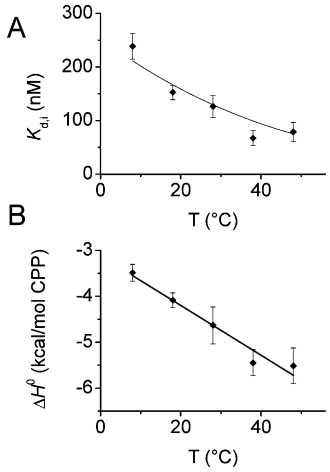

FIGURE 2: Dissociation constant and reaction enthalpy as a function of the temperature for Tat-PTD binding to DNA. (A) Dissociation constant $K_{d,i}$ versus the temperature. Solid line is the predicted temperature dependence of $K_{d,i}$ using the (◆) measured temperature dependence of ΔH^0 and the van't Hoff relation $d \ln K/dT = \Delta H^0/RT^2$. (B) ΔH^0_{CPP} versus the temperature, where (◆) experimental values and the solid line represents linear regression analysis, yielding ΔH^0_{CPP} (kcal/mol CPP) = $-0.0542T$ (°C) − 3.1169 and thus a negative heat capacity change of ΔC^0_p of −54.2 cal (mol of peptide)$^{-1}$ K^{-1}.

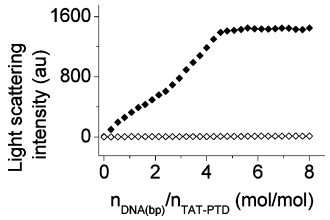

FIGURE 3: Clustering of DNA with Tat-PTD as evidenced by static right-angle light scattering. The optical cuvette is filled with 1.4 mL of either (◆) 50 μM Tat-PTD or (◇) buffer. Every 5 min, 10 μL of 1.87 mM (bp) DNA is added under constant stirring. The buffer was 30 mM phosphate and 76 mM NaCl at pH 7.40 (resulting in an ionic strength of 154 mM), and the temperature was 25 °C.

reaction is dominated by changes in solvent-accessible surface area (dehydration). In contrast, a positive heat capacity generally indicates that the reaction is driven by an electrostatic interaction such as observed for charge neutralization of DNA with smaller cations such as trivalent cobalt hexammine (*24*).

The change in solvent-accessible surface and the formation of DNA complexes with the CPP is supported indirectly by static light scattering (Figure 3). In these experiments, 1.4 mL of a 50.0 μM solution of the CPP was titrated every 5 min with 10 μL of a 1.87 mM (bp) DNA solution. During the initial 17 injections, the intensity of scattered light continuously increased, which is consistent with the observation that DNA compaction occurs when more than 90% of the DNA phosphate charge is neutralized (*31*), as is the case during the initial injections. A maximum of scattering was observed at a DNA(bp)/Tat-PTD molar ratio of $r_{DNA/CPP} \approx 4$, indicating that no further CPP−DNA complex formation occurred after charge neutralization in agreement with the ITC data. Comparable DNA aggregates with polycations have been termed polyplexes or DNA condensates depending upon their composition, size, and morphology (*32*). Present observations, however, contrast the binding of smaller cations as trivalent cobalt hexammine or spermidine to DNA that are characterized by a positive reaction enthalpy, a predominant contribution of entropy to the binding reaction, and a much weaker DNA condensing capacity (*24*, *33*).

Fluorescence. The high affinity of the CPP for DNA suggests that CPPs may bind to intracellular DNA after cellular/nuclear uptake. This is evidenced by fluorescence microscope observations, where an intense signal of fluorescently labeled CPPs has been observed in the nucleus of living cells (*5*). The observed fluorescence intensity, however, will depend upon several factors and might be influenced by the mode of CPP binding and the physiological conditions encountered in the different cellular organelles. We were thus interested in whether the bright fluorescence intensity in the cell nucleus indeed reflects the nuclear accumulation of the CPP or whether it is caused by an increased quantum yield of the fluorescent dye during the interaction of the CPP with DNA. Such an enhancement of the quantum yield is known from other DNA-binding molecules such as ethidium bromide, where the signal is enhanced up to 40 times when interacting with DNA (for a review, see ref *34*).

In the present experiments, the signal of the fluorescent CPP is not enhanced during the interaction with DNA but decreases to 51.2 ± 0.3% of its original value in buffer when saturated with DNA (Figure 4C). This indicates that the correlation between the CPP concentration and fluorescence intensity is not linear. In the fluorescence microscope, the actual CPP concentration in the nucleus may thus be underestimated by a factor of up to 2 with respect to the extracellular label.

Even more dramatic changes were observed when fluorescently labeled CPP interacted with GAGs, the likely mediators of the CPP uptake (*26*−*28*). Under comparable conditions, the same absolute amount of fluorescent CPP produced only 15.3 ± 0.7% of its initial value in buffer, when the CPP was saturated with GAGs (Figure 4D).

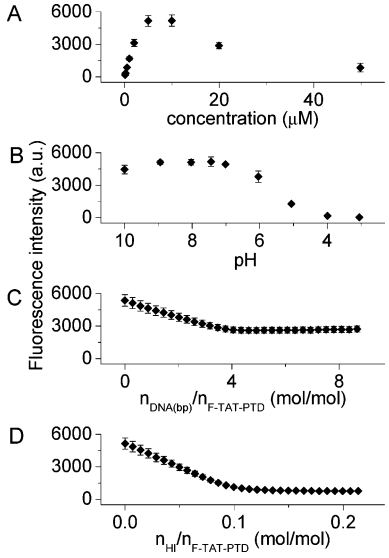

FIGURE 4: Fluorescence intensity of FITC-labeled Tat-PTD as (A) a function of its bulk concentration, (B) 5 μM Tat-PTD at variable pH, (C) 5 μM Tat-PTD with increasing amounts of DNA, (D) 5 μM Tat-PTD with increasing amounts of GAGs. The same *y* scale is used in all panels ($\lambda_{em}/\lambda_{ex}$ = 498/521 nm). (A) FITC-labeled HIV Tat-PTD at different concentrations suggests pronounced self-quenching at concentrations above 5 μM. (B) FITC-labeled HIV Tat-PTD at a constant concentration (5 μM) but varying pH (phosphate buffer), illustrating that the acidic pH leads to an extensive loss of the fluorescence signal. To measure the effects of ligand binding on the fluorescence signal, 1.4 mL of 5 μM fluorescently labeled HIV Tat-PTD was titrated every 5 min under constant stirring with either 10 μL of (C) 0.203 mM (bp) DNA or (D) 4.99 μM heparin. The buffer in all experiments was 30 mM phosphate and 76 mM NaCl at pH 7.40 (resulting in an ionic strength of 154 mM), and the temperature was 25 °C.

Considering that most of the reduction in fluorescence intensity is caused by self-quenching between proximate fluorescein molecules (*35*) in present multisite binding reaction, the more pronounced fluorescence quenching with GAGs suggests that CPPs are tighter packed when bound to heparin than with DNA. This is also supported by the more negative reaction enthalpy (*29*), which is commonly related to the release of hydration water in polyelectrolyte interactions (*31*).

At pH 5 and 4 (Figure 4B), the fluorescence intensity of the labeled CPP was reduced to 24.8 ± 0.6 and even 3.4 ± 0.2%, respectively, as compared to its value at physiological pH of 7.4. This observation is of high relevance for CPP investigations in living cells, because the CPPs on their assumed uptake route via endosomes (*36*) experience a distinct pH decrease (*37*).

A major decrease of the fluorescence intensity was also observed when the label concentration was higher than 5 μM (Figure 4A), a condition likely to occur *in vivo*. CPPs are commonly administered to living cells in this concentration range, which then may be further increased by accumulation in cellular organelles. The concentration for self-quenching of the labeled CPP is thus close to that reported for pure FITC in solution (*38*). Present findings therefore suggest that a quantitative analysis of the cellular CPP concentration based on fluorescence intensity data alone (e.g., confocal microscopy or FACS) is rather difficult, because of the nonlinear relationship between the CPP concentration and fluorescence signal at various (sub)cellular conditions. The situation can be aggravated by fluorescence quenching. A reduction in the fluorescence intensity might also result from precipitation out of the (confocal) plane of detection, if stirring is absent.

DISCUSSION

Binding Affinity. Present results demonstrate that the 11-residue basic epitope (amino acids 49−57) of HIV-1 Tat binds with high affinity to double-stranded DNA with a dissociation constant of $K_d \approx 100$ nM (Figure 2). This is in stark contrast to the transfection reagent PLL (*2*), where a minimum chain length of 20 amino acids is required for DNA binding (*32*). Interestingly, the observed dissociation constant for binding of HIV-1 Tat-PTD to DNA (Table 1) is only slightly higher than reported for the *specific* interaction of the full-length HIV-1 Tat to TAR (*18*). At 37 °C, the K_d values of the two processes are even identical (60−70 nM). This high DNA-binding affinity confers stability to the uptake complexes of *extracellular* DNA and CPPs but also points to the potential interference of the CPP with *intracellular* DNA and also the competitive release of the cargo after cellular uptake. The high affinity of HIV Tat-PTD for DNA *in vitro* is consistent with fluorescence microscope studies *in vivo*, where the fluorescence intensity of the CPP was found to be associated predominantly with the cell nucleus (*5*), suggesting potential binding of the CPP to the genome. The fast accumulation of the CPP in the nucleus might also be a consequence of the structural analogy of CPPs with nuclear localization signals (NLSs) because the latter commonly contain one or more clusters of basic amino acids for the interaction with importins. The accumulation of the CPP in the nucleus is of particular interest for transfection assays, because the nucleus is commonly the intended target location for the transported nucleotides.

To the best of our knowledge, no binding parameters for the interaction of DNA with HIV-1 Tat have been reported to date. Nonetheless, present findings on the high affinity of the HIV-1 Tat-PTD for DNA are in good agreement with earlier observations for the full-length Tat protein from the equine infectious anemia virus (EIAV). EIAV Tat binds to EIAV TAR with only low affinity (millimolar range) but has a high affinity for DNA ($K_d \approx 100$ nM) (*39*).

It could be argued that, under *in vivo* conditions, the CPP binding to DNA involves specific recognition sites such as known for HIV-1 TAR or aptamers. The reaction stoichiometry equal to charge neutrality, however, suggests that the CPP interacts with the backbone of the DNA (i.e., phosphate groups) rather than specifically with distinct base pairs. In analogy, the interaction of oligoarginine with homologue oligonucleotides is characterized by a similar affinity and stoichiometry as observed here (*14*), supporting the view that oligocation interactions with DNA possess not only a high affinity but also a high structural flexibility (*14*). Such polyvalent electrostatic interactions are commonly accompanied by DNA condensation and intermolecular cross-linking. This electrostatic mechanism is quite different from site-specific DNA recognition primarily governed by hydrogen bonding to DNA bases (*40*).

Knowing the affinity of CPPs for DNA and other cellular molecules allows us to estimate the stability of the transport

complex before, during, and after the prospective cellular uptake. For uptake, for example, the complex requires the presence of GAGs on the cell surface (*26*, *27*). The complex must also bear a residual positive charge for optimum uptake yield (*4*). The present experiments suggest that this requirement for a residual positive charge of the CPP−DNA complex is a consequence of the lower affinity of the peptide for GAGs (*29*) than for DNA (Table 1). Apparently, GAGs cannot break up the CPP−DNA interaction. They leave the transport complex intact and therefore require residual positive charges for additional interactions to take place. The residual positive charge also seems beneficial in stabilizing the complexes in solution (*41*).

Toxicity. The discovery and characterization of cell-penetrating compounds, such as PLL, polyethylenimine, cationic lipids, and CPPs have been regarded as a hallmark for delivering genes and drugs to biological cells by nonviral means (*1*−*3*, *42*). Because the application of CPPs in medical therapies seems very attractive, more must be known about the uptake route of CPPs, and only a few studies have focused on the safety of these compounds. Most toxicity studies have addressed the acute toxicity of CPPs on a time scale in the minute to hour range, but results are inconsistent. On the one hand, it has been concluded that these compounds have a low or no acute toxicity (*6*−*8*). On the other hand, it has been observed that CPPs have a pronounced acute toxicity (*9*−*11*), ranging from reduced viability in the cell culture (*43*) to aggregations in cell suspensions (*44*) and cell agglutination (*45*).

Even less is known about the long-term toxicity of CPPs with a specific focus on the interaction with the genome of the host. The Tat binding to DNA as demonstrated here may affect the DNA superstructure, the binding sites for growth and transcription factors and thus, in turn, the RNA/protein synthesis. While the binding of polyamines to DNA might be protective, because the condensed physical state apparently reduces harmful effects of reactive oxygen species (*46*), it can also be toxic (*9*, *47*, *48*) and in rare cases even mutagenic (*49*). Further studies are thus essential to understand the potential and the risks of CPP applications.

Fluorescence. Various research studies aim at clarifying and comparing uptake efficiency and subcellular routes of different cell-penetrating reagents by fluorescent means. In this context, a punctuate pattern of fluorescent CPPs in cells has been generally assigned to endosomal uptake, whereas a diffuse staining is considered a sign of membrane instability and pore formation (*10*, *50*, *51*). Conclusions on their uptake mechanism, however, are inconsistent (*10*, *42*, *50*, *52*−*54*), and some of the difficulties have been already elucidated (*50*, *51*, *55*, *56*).

Our studies illustrate that such conflicting results may arise from considerable changes in the fluorescence quantum yield depending upon the (sub)cellular conditions and the types of fluorophores used. In particular, cellular polyanions such as GAGs and DNA contain multiple binding sites for labeled CPPs, thereby affecting the fluorescence quantum yield of the closely packed fluorophores. Additionally, condensation of the molecules takes place. The change in the fluorescence quantum yield and the extent of condensation depend upon the particular CPP and the molecular nature of the polyanion (Figure 4) and are furthermore subject to change along the uptake route. In this respect, the fluorescence signal is affected by internal quenching, if the probe reaches a critical limit in solution and in multisite binding reactions. For fluorescein, for example, the critical intermolecular distance for self-quenching has been estimated to be on the order of 50 Å (*35*). The relatively high pK_a of 6.4 for FITC (*57*) might also explain the extensive changes in the fluorescence signal when the pH varies within the physiological range (Figure 4). These observations are of particular relevance for the observation of CPPs, because the pH in the nucleoplasm is generally 0.3−0.5 units above that of the cytosplasm (*58*), whereas the pH in endosomes is between 4.6 and 5.0 (*37*). On the basis of the fluorescent signals alone, the concentration of CPPs in acid organelles might thus be heavily underestimated.

The observed nonlinearity between the fluorescence intensity and CPP concentration therefore impedes the quantitative interpretation of fluorescent microscope images and FACS. The self-quenching property, however, can also be exploited for the time-lapse observation in living cells. Accordingly, the signal of low concentrations of intracellular CPP can be enhanced with respect to the extracellular fluorescence by quenching the external dye at concentrations above 5 μM (*5*).

CONCLUSIONS

Knowledge of the binding affinity of CPPs for GAGs, cellular DNA, and transported cargos contributes to a better understanding of the delicate balance between the stability of the uptake complex, need of distinct molar ratios for optimum uptake yield, and intracellular release of the cargo. In addition, the strong DNA-binding affinity of CPPs could influence the superstructure and expression of the host's genome, which must be addressed in toxicity studies. The interaction of CPPs with biological polyanions such as DNA and GAGs essentially leads to condensation of the reactants, thereby strongly affecting the fluorescence signal of the labeled CPP. This is important when comparing uptake efficiencies of different fluorescent CPPs and elucidating their subcellular routes by fluorescent means.

REFERENCES

1. Schwarze, S. R., Hruska, K. A., and Dowdy, S. F. (2000) Protein transduction: Unrestricted delivery into all cells? *Trends Cell Biol. 10*, 290−295.
2. Ryser, H. J., and Hancock, R. (1965) Histones and basic polyamino acids stimulate the uptake of albumin by tumor cells in culture, *Science 150*, 501−503.
3. Boussif, O., Lezoualc'h, F., Zanta, M. A., Mergny, M. D., Scherman, D., Demeneix, B., and Behr, J. P. (1995) A versatile vector for gene and oligonucleotide transfer into cells in culture and in vivo: Polyethylenimine, *Proc. Natl. Acad. Sci. U.S.A. 92*, 7297−7301.
4. Choosakoonkriang, S., Lobo, B. A., Koe, G. S., Koe, J. G., and Middaugh, C. R. (2003) Biophysical characterization of PEI/DNA complexes, *J. Pharm. Sci. 92*, 1710−1722.
5. Ziegler, A., Nervi, P., Durrenberger, M., and Seelig, J. (2005) The cationic cell-penetrating peptide CPP(TAT) derived from the HIV-1 protein TAT is rapidly transported into living fibroblasts: Optical, biophysical, and metabolic evidence, *Biochemistry 44*, 138−148.
6. Jones, S. W., Christison, R., Bundell, K., Voyce, C. J., Brockbank, S. M., Newham, P., and Lindsay, M. A. (2005) Characterisation of cell-penetrating peptide-mediated peptide delivery, *Br. J. Pharmacol. 145*, 1093−1102.

7. Trehin, R., Krauss, U., Muff, R., Meinecke, M., Beck-Sickinger, A. G., and Merkle, H. P. (2004) Cellular internalization of human calcitonin derived peptides in MDCK monolayers: A comparative study with Tat(47−57) and penetratin(43−58), *Pharm. Res. 21*, 33−42.
8. Vives, E., Brodin, P., and Lebleu, B. (1997) A truncated HIV-1 Tat protein basic domain rapidly translocates through the plasma membrane and accumulates in the cell nucleus, *J. Biol. Chem. 272*, 16010−16017.
9. Kornguth, S. E., Stahmann, M. A., and Anderson, J. W. (1961) Effect of polylysine on the cytology of Ehrlich ascites tumor cells, *Exp. Cell Res. 24*, 484−494.
10. Mano, M., Teodosio, C., Paiva, A., Simoes, S., and Pedroso de Lima, M. C. (2005) On the mechanisms of the internalization of S4(13)-PV cell-penetrating peptide, *Biochem. J. 390*, 603−612.
11. Saar, K., Lindgren, M., Hansen, M., Eiriksdottir, E., Jiang, Y., Rosenthal-Aizman, K., Sassian, M., and Langel, U. (2005) Cell-penetrating peptides: A comparative membrane toxicity study, *Anal. Biochem. 345*, 55−65.
12. Mann, D. A., and Frankel, A. D. (1991) Endocytosis and targeting of exogenous HIV-1 Tat protein, *EMBO J. 10*, 1733−1739.
13. Rana, T. M., and Jeang, K.-T. (1999) Biochemical and functional interactions between HIV-1 Tat protein and TAR RNA, *Arch. Biochem. Biophys. 365*, 175−185.
14. Calnan, B. J., Biancalana, S., Hudson, D., and Frankel, A. D. (1991) Analysis of arginine-rich peptides from the HIV Tat protein reveals unusual features of RNA−protein recognition, *Genes Dev. 5*, 201−210.
15. Kamine, J., Loewenstein, P., and Green, M. (1991) Mapping of HIV-1 Tat protein sequences required for binding to Tar RNA, *Virology 182*, 570−577.
16. Karn, J., Dingwall, C., Finch, J. T., Heaphy, S., and Gait, M. J. (1991) RNA binding by the Tat and Rev proteins of HIV-1, *Biochimie 73*, 9−16.
17. Slice, L. W., Codner, E., Antelman, D., Holly, M., Wegrzynski, B., Wang, J., Toome, V., Hsu, M. C., and Nalin, C. M. (1992) Characterization of recombinant HIV-1 Tat and its interaction with TAR RNA, *Biochemistry 31*, 12062−12068.
18. Metzger, A. U., Bayer, P., Willbold, D., Hoffmann, S., Frank, R. W., Goody, R. S., and Rosch, P. (1997) The interaction of HIV-1 Tat(32−72) with its target RNA: A fluorescence and nuclear magnetic resonance study, *Biochem. Biophys. Res. Commun. 241*, 31−36.
19. Weeks, K. M., Ampe, C., Schultz, S. C., Steitz, T. A., and Crothers, D. M. (1990) Fragments of the HIV-1 Tat protein specifically bind TAR RNA, *Science 249*, 1281−1285.
20. Lundback, T., and Hard, T. (1996) Sequence-specific DNA-binding dominated by dehydration, *Proc. Natl. Acad. Sci. U.S.A. 93*, 4754−4759.
21. van Holde, K. E., Johnson, W. C., and Ho, P. S. (1998) Chemical equilibria involving macromolecules, in *Principles of Physical Biochemistry* (van Holde, K. E., Johnson, W. C., and Ho, P. S., Eds.) 1st ed., pp 605−611, Prentice Hall, Upper Saddle River, NJ.
22. Dizhe, E. B., Ignatovich, I. A., Burov, S. V., Pohvoscheva, A. V., Akifiev, B. N., Efremov, A. M., Perevozchikov, A. P., and Orlov, S. V. (2006) Complexes of DNA with cationic peptides: Conditions of formation and factors effecting internalization by mammalian cells, *Biochemistry (Moscow) 71*, 1350−1356.
23. Ross, P. D., and Shapiro, J. T. (1974) Heat of interaction of DNA with polylysine, spermine, and Mg^{2+}, *Biopolymers 13*, 415−416.
24. Matulis, D., Rouzina, I., and Bloomfield, V. A. (2000) Thermodynamics of DNA binding and condensation: Isothermal titration calorimetry and electrostatic mechanism, *J. Mol. Biol. 296*, 1053−1063.
25. Mascotti, D. P., and Lohman, T. M. (1997) Thermodynamics of oligoarginines binding to RNA and DNA, *Biochemistry 36*, 7272−7279.
26. Williams, K. J., and Fuki, I. V. (1997) Cell-surface heparan sulfate proteoglycans: Dynamic molecules mediating ligand catabolism, *Curr. Opin. Lipidol. 8*, 253−262.
27. Tyagi, M., Rusnati, M., Presta, M., and Giacca, M. (2001) Internalization of HIV-1 Tat requires cell surface heparan sulfate proteoglycans, *J. Biol. Chem. 276*, 3254−3261.
28. Ziegler, A., Blatter, X. L., Seelig, A., and Seelig, J. (2003) Protein transduction domains of HIV-1 and SIV TAT interact with charged lipid vesicles. Binding mechanism and thermodynamic analysis, *Biochemistry 42*, 9185−9194.
29. Ziegler, A., and Seelig, J. (2004) Interaction of the protein transduction domain of HIV-1 TAT with heparan sulfate: Binding mechanism and thermodynamic parameters, *Biophys. J. 86*, 254−263.
30. Ziegler, A., and Zaia, J. (2006) Size-exclusion chromatography of heparin oligosaccharides at high and low pressure, *J. Chromatogr., B: Biomed. Sci. Appl. 837*, 76−86.
31. Kankia, B. I., Buckin, V., and Bloomfield, V. A. (2001) Hexamminecobalt(III)-induced condensation of calf thymus DNA: Circular dichroism and hydration measurements, *Nucleic Acids Res. 29*, 2795−2801.
32. Kwoh, D. Y., Coffin, C. C., Lollo, C. P., Jovenal, J., Banaszczyk, M. G., Mullen, P., Phillips, A., Amini, A., Fabrycki, J., Bartholomew, R. M., Brostoff, S. W., and Carlo, D. J. (1999) Stabilization of poly-L-lysine/DNA polyplexes for in vivo gene delivery to the liver, *Biochim. Biophys. Acta 1444*, 171−190.
33. Widom, J., and Baldwin, R. L. (1983) Monomolecular condensation of λ-DNA induced by cobalt hexamine, *Biopolymers 22*, 1595−1620.
34. Olmsted, J., III, and Kearns, D. R. (1977) Mechanism of ethidium bromide fluorescence enhancement on binding to nucleic acids, *Biochemistry 16*, 3647−3654.
35. Kawski, A. (1983) Excitation energy transfer and its manifestation in isotropic media, *Photochem. Photobiol. 38*, 487−508.
36. Melikov, K., and Chernomordik, L. V. (2005) Arginine-rich cell penetrating peptides: From endosomal uptake to nuclear delivery, *Cell. Mol. Life Sci. 62*, 2739−2749.
37. Mellman, I., Fuchs, R., and Helenius, A. (1986) Acidification of the endocytic and exocytic pathways, *Annu. Rev. Biochem. 55*, 663−700.
38. Schauenstein, K., Schauenstein, E., and Wick, G. (1978) Fluorescence properties of free and protein bound fluorescein dyes. I. Macrospectrofluorometric measurements, *J. Histochem. Cytochem. 26*, 277−283.
39. Willbold, D., Metzger, A. U., Sticht, H., Gallert, K. C., Voit, R., Dank, N., Bayer, P., Krauss, G., Goody, R. S., and Rosch, P. (1998) Equine infectious anemia virus transactivator is a homeodomain-type protein, *J. Mol. Biol. 277*, 749−755.
40. Mandel-Gutfreund, Y., Schueler, O., and Margalit, H. (1995) Comprehensive analysis of hydrogen bonds in regulatory protein DNA-complexes: In search of common principles, *J. Mol. Biol. 253*, 370−382.
41. Clamme, J. P., Azoulay, J., and Mely, Y. (2003) Monitoring of the formation and dissociation of polyethylenimine/DNA complexes by two photon fluorescence correlation spectroscopy, *Biophys. J. 84*, 1960−1968.
42. Lindgren, M., Hallbrink, M., Prochiantz, A., and Langel, U. (2000) Cell-penetrating peptides, *Trends Pharmacol. Sci. 21*, 99−103.
43. Choi, Y. H., Liu, F., Choi, J. S., Kim, S. W., and Park, J. S. (1999) Characterization of a targeted gene carrier, lactose-polyethylene glycol-grafted poly-L-lysine and its complex with plasmid DNA, *Hum. Gene Ther. 10*, 2657−2665.
44. Katchalsky, A., Danon, D., and Nevo, A. (1959) Interactions of basic polyelectrolytes with the red blood cell. II. Agglutination of red blood cells by polymeric bases, *Biochim. Biophys. Acta 33*, 120−138.
45. Matsuya, Y., and Yamane, I. (1985) Cell hybridization and cell agglutination. II. Enhancement of cell hybridization by polycations, *J. Cell Sci. 78*, 273−282.
46. Pedreno, E., Lopez-Contreras, A. J., Cremades, A., and Penafiel, R. (2005) Protecting or promoting effects of spermine on DNA strand breakage induced by iron or copper ions as a function of metal concentration, *J. Inorg. Biochem. 99*, 2074−2080.
47. Hunter, A. C. (2006) Molecular hurdles in polyfectin design and mechanistic background to polycation induced cytotoxicity, *Adv. Drug Delivery Rev. 58*, 1523−1531.
48. Richardson, T., Hodgett, J., Lindner, A., and Stahmann, M. A. (1959) Action of polylysine on some ascites tumors in mice, *Proc. Soc. Exp. Biol. Med. 101*, 382−386.
49. Ferguson, L. R., and Baguley, B. C. (1981) The relationship between frameshift mutagenicity and DNA-binding affinity in a series of acridine-substituted derivatives of the experimental antitumour drug 4′-(9-acridinylamino)methanesulphonanilide (AMSA), *Mutat. Res. 82*, 31−39.
50. Thoren, P. E., Persson, D., Isakson, P., Goksor, M., Onfelt, A., and Norden, B. (2003) Uptake of analogs of penetratin, Tat(48−60) and oligoarginine in live cells, *Biochem. Biophys. Res. Commun. 307*, 100−107.

51. Tunnemann, G., Martin, R. M., Haupt, S., Patsch, C., Edenhofer, F., and Cardoso, M. C. (2006) Cargo-dependent mode of uptake and bioavailability of TAT-containing proteins and peptides in living cells, *FASEB J. 20*, 1775−1784.
52. Drin, G., Cottin, S., Blanc, E., Rees, A. R., and Temsamani, J. (2003) Studies on the internalization mechanism of cationic cell-penetrating peptides, *J. Biol. Chem. 278*, 31192−31201.
53. Fischer, R., Kohler, K., Fotin-Mleczek, M., and Brock, R. (2004) A stepwise dissection of the intracellular fate of cationic cell-penetrating peptides, *J. Biol. Chem. 279*, 12625−12635.
54. Fretz, M. M., Penning, N. A., Taei, S. A., Futaki, S., Takeuchi, T., Nakase, I., Storm, G., and Jones, A. T. (2007) Temperature, concentration and cholesterol dependent translocation of L- and D-octaarginine across the plasma and nuclear membrane of CD34 + leukaemia cells, *Biochem. J. 403*, 335−342.
55. Vives, E., Richard, J. P., Rispal, C., and Lebleu, B. (2003) TAT peptide internalization: Seeking the mechanism of entry, *Curr. Protein Pept. Sci. 4*, 125−132.
56. Szeto, H. H., Schiller, P. W., Zhao, K., and Luo, G. (2005) Fluorescent dyes alter intracellular targeting and function of cell-penetrating tetrapeptides, *FASEB J. 19*, 118−120.
57. Sjoback, R., Nygren, J., and Kubista, M. (1998) Characterization of fluorescein-oligonucleotide conjugates and measurement of local electrostatic potential, *Biopolymers 46*, 445−453.
58. Seksek, O., and Bolard, J. (1996) Nuclear pH gradient in mammalian cells revealed by laser microspectrofluorimetry, *J. Cell Sci. 109* (part 1), 257−262.

BI700416H